

Unsaturated Binuclear Cyclopentadienylrhenium Carbonyl Derivatives: Metal–Metal Multiple Bonds and Agostic Hydrogen Atoms

Bing Xu,[†] Qian-shu Li,^{†,‡} Yaoming Xie,[§] R. Bruce King,^{*,‡,§} and Henry F. Schaefer III[§]

Institute of Chemical Physics, Beijing Institute of Technology, Beijing 100081, P.R. China, Center for Computational Quantum Chemistry, School of Chemistry and Environment, South China Normal University, Guangzhou 510631, P.R. China, and Department of Chemistry and Center for Computational Chemistry, University of Georgia, Athens, Georgia 30602

Received March 5, 2008

The cyclopentadienylrhenium carbonyls $\text{Cp}_2\text{Re}_2(\text{CO})_n$ ($\text{Cp} = \eta^5\text{-C}_5\text{H}_5$; $n = 5, 4, 3, 2$) have been studied by density functional theory. The global minima for the $\text{Cp}_2\text{Re}_2(\text{CO})_n$ ($n = 5, 4, 3, 2$) derivatives are predicted to be the singly bridged structure $\text{Cp}_2\text{Re}_2(\text{CO})_4(\mu\text{-CO})$ with a formal Re–Re single bond; the doubly semibridged structure $\text{Cp}_2\text{Re}_2(\text{CO})_4$ with a formal Re=Re double bond; the triply bridged structure $\text{Cp}_2\text{Re}_2(\mu\text{-CO})_3$ with a formal Re≡Re triple bond; and the doubly bridged structure $\text{Cp}_2\text{Re}_2(\mu\text{-CO})_2$, respectively. The first three of these predicted structures have been realized experimentally in the stable compounds $(\eta^5\text{-C}_5\text{H}_5)_2\text{Re}_2(\text{CO})_4(\mu\text{-CO})$, $(\eta^5\text{-Me}_5\text{C}_5)_2\text{Re}_2(\text{CO})_4$ and $(\eta^5\text{-Me}_5\text{C}_5)_2\text{Re}_2(\mu\text{-CO})_3$. In addition, structures of the type $\text{Cp}_2\text{Re}-\text{Re}(\text{CO})_n$ with both rings bonded only to one metal and unknown in manganese chemistry are also found for rhenium but at energies significantly above the global minima. The unsaturated $\text{Cp}_2\text{Re}-\text{Re}(\text{CO})_n$ structures ($n = 4, 3, 2$) have agostic Cp hydrogen atoms forming C–H–Re bridges to the unsaturated $\text{Re}(\text{CO})_n$ group with a Re–H distance as short as 2.04 Å.

1. Introduction

Three general structure types are, in principle, possible for binuclear cyclopentadienylmetal carbonyls, $\text{Cp}_2\text{M}_2(\text{CO})_n$ ($\text{Cp} = \text{cyclopentadienyl}$ or substituted cyclopentadienyl), depending on whether each metal is bonded to a single Cp ring (**I** in Figure 1), whether the two Cp rings bridge the pair of metal atoms (**II** in Figure 1), or whether one of the metals is bonded to both Cp rings and the second metal is bonded only to carbonyl groups (**III** in Figure 1). In this connection all of the known binuclear cyclopentadienylmetal carbonyls such as $\text{Cp}_2\text{Cr}_2(\text{CO})_6$, $\text{Cp}_2\text{Fe}_2(\text{CO})_4$, and $\text{Cp}_2\text{Ni}_2(\text{CO})_2$ have structures in which each metal atom is bonded to a single Cp ring (**I** in Figure 1). In addition, our previous density functional theory (DFT) studies found some $(\mu\text{-Cp})_2\text{M}_2(\text{CO})_n$ structures for the relatively late transition metals iron,¹ cobalt,² and nickel³ in which both Cp rings

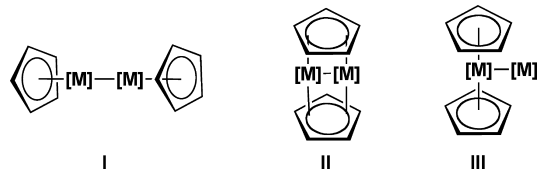


Figure 1. Three general structure types for binuclear cyclopentadienylmetal carbonyls, $\text{Cp}_2\text{M}_2(\text{CO})_n$ where [M]–[M] refers to a bonded pair of metal atoms with associated CO groups.

bridge the pair of metal atoms (**II** in Figure 1). However, such structures are of significantly higher energy and apparently limited to a maximum of two carbonyl groups, at least for the first row transition metals studied to date. This is probably why such structures, even as theoretical relatively high-energy alternatives, have at least so far been found only toward the end of the transition series. The third alternative (**III** in Figure 1), namely structures of the type $\text{Cp}_2\text{M}-\text{M}(\text{CO})_n$ in which both Cp rings are bonded only to one of the metals, does not appear to have been considered either experimentally or theoretically other than trivial cases of ionic derivatives such as $\text{Cp}_2\text{Co}^+\text{Co}(\text{CO})_4^-$ with no

* To whom correspondence should be addressed. E-mail: rbking@chem.uga.edu.

[†] Beijing Institute of Technology.

[‡] South China Normal University.

[§] University of Georgia.

(1) Wang, H. Y.; Xie, Y.; King, R. B.; Schaefer, H. F. *Inorg. Chem.* **2006**, *45*, 3384.

(2) Wang, H.; Xie, Y.; King, R. B.; Schaefer, H. F. *J. Am. Chem. Soc.* **2005**, *127*, 11646.

(3) Wang, H.; Xie, Y.; King, R. B.; Schaefer, H. F. *Inorg. Chem.* **2006**, *45*, 5621.

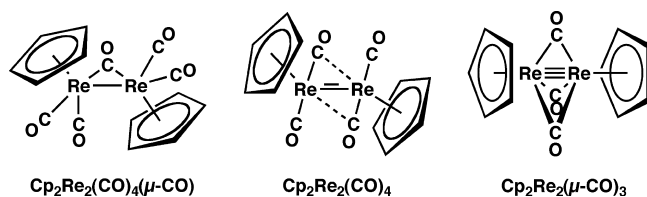


Figure 2. Structures of $\text{Cp}_2\text{Re}_2(\text{CO})_n$ derivatives that have been isolated and characterized by X-ray diffraction. Substituents on the Cp rings are omitted for clarity.

covalent chemical bonding between the Cp_2Co^+ cation and the $\text{Co}(\text{CO})_4^-$ anion.

The third row transition metal rhenium is a particularly interesting candidate for unusual binuclear cyclopentadienylrhenium carbonyls $\text{Cp}_2\text{Re}_2(\text{CO})_n$ for a number of reasons. First, the stability of Cp_2ReH and other Cp_2ReX derivatives ($X = \text{halogen, alkyl, etc.}$)^{4–6} suggests the possible existence of $\text{Cp}_2\text{Re}–\text{Re}(\text{CO})_n$ structural isomers for $\text{Cp}_2\text{Re}_2(\text{CO})_n$ (i.e., **III** in Figure 1). Furthermore, binuclear cyclopentadienylrhenium carbonyl derivatives of several types are relatively stable, as indicated by the isolation of $(\eta^5\text{-C}_5\text{H}_5)_2\text{Re}_2(\text{CO})_4(\mu\text{-CO})$ (ref 7), $(\eta^5\text{-Me}_5\text{C}_5)_2\text{Re}_2(\text{CO})_4$ (ref 8), and $(\eta^5\text{-Me}_5\text{C}_5)_2\text{Re}_2(\mu\text{-CO})_3$ (ref 9) with formal single, double, and triple metal–metal bonds, respectively, as sufficiently stable compounds for structure determination by X-ray crystallography (Figure 2). This suggests that interesting new compounds predicted by the present theoretical study on $\text{Cp}_2\text{Re}_2(\text{CO})_n$ derivatives have a reasonable chance of being realized experimentally, possibly as stable isolable compounds. Also, the first formal metal–metal quadruple bond was found by Cotton and Harris¹⁰ in the now famous binuclear halide $[\text{Cl}_4\text{ReReCl}_4]^{2-}$. This suggests that highly unsaturated binuclear $\text{Cp}_2\text{Re}_2(\text{CO})_n$ derivatives might be interesting new candidates exhibiting high order metal–metal multiple bonding^{11,12} leading to interesting chemical reactivity patterns.

This paper presents DFT studies on the series of binuclear cyclopentadienylrhenium carbonyls $\text{Cp}_2\text{Re}_2(\text{CO})_n$ ($n = 5, 4, 3, 2$) corresponding to structures requiring formal rhenium–rhenium bonds of orders 1, 2, 3, and 4, respectively, if the 18-electron rule is followed and there are no four-electron donor bridging carbonyl groups. This work, which is the first comprehensive DFT study of $\text{Cp}_2\text{M}_2(\text{CO})_n$ derivatives of a second or third row transition metal, provides the first examples of structures of the type $\text{Cp}_2\text{M}–\text{M}(\text{CO})_n$ (**III** in Figure 1: $\text{M}=\text{Re}$ in this case). The binuclear structures $\text{Cp}_2\text{Re}–\text{Re}(\text{CO})_n$ are particularly interesting, since the 17-electron Cp_2Re structural unit can only form a single bond with a $\text{Re}(\text{CO})_n$ unit without exceeding the favored 18-electron configuration or leading to dipolar structures. For

this reason unsaturated structures of the type $\text{Cp}_2\text{Re}–\text{Re}(\text{CO})_n$ ($n = 4, 3, 2$), arising for the first time in the theoretical studies reported here, introduce a feature new to cyclopentadienylmetal carbonyl chemistry, namely, one or more agostic hydrogen atoms in the Cp rings forming $\text{C}–\text{H}–\text{Re}$ three-center bonds to the unsaturated $\text{Re}(\text{CO})_n$ site.

2. Theoretical Methods

Electron correlation effects were considered by employing DFT, which has evolved as a practical and effective computational tool especially for organometallic compounds.^{13–21} In this work, the two DFT methods BP86 and MPW1PW91 were used. The BP86 method is a pure DFT method combining Becke's 1988 exchange functional with Perdew's 1986 correlation functional^{22,23} The MPW1PW91 method²⁴ is a so-called second-generation²⁵ functional, namely a combination of the modified Perdew–Wang exchange functional with the Perdew–Wang 91 gradient–correlation functional.²⁶ The MPW1PW91 method has been found to be more suitable for geometry optimization of the second and third row transition metal systems while the BP86 method usually provides better vibrational frequencies.^{27,28}

For the third row transition metals, the large numbers of electrons can increase exponentially the computational efforts. To reduce the cost, effective core potential (ECP) basis sets were employed, which include relativistic effects. In this study the SDD (Stuttgart–Dresden ECP plus DZ),²⁹ ECP basis set was used for the rhenium atoms. For the C and O atoms, the double- ζ plus polarization (DZP) basis sets were used. They are the Huzinaga–Dunning contracted double- ζ contraction sets^{30,31} plus a set of spherical harmonic d polarization functions with orbital exponents $\alpha_d(\text{C}) = 0.75$ and $\alpha_d(\text{O}) = 0.85$ and designated as (9s5p1d/4s2p1d). For H, a set of p polarization functions, $\alpha_p(\text{H}) = 0.75$, was added to the Huzinaga–Dunning DZ set.

The geometries of all structures were fully optimized using the two selected DFT methods along with the SDD ECP basis set. Vibrational frequencies were determined by evaluating analytically the second derivatives of the energy with respect to the nuclear coordinates at the same levels. The corresponding infrared intensities were also evaluated analytically. All of the computations were carried out with the Gaussian 03 program.³² The fine grid (75, 302)

- (4) Apostolidis, C.; Kannelakopoulos, B.; Maier, R.; Rebizant, J.; Ziegler, M. L. *J. Organomet. Chem.* **1991**, *409*, 243.
 (5) Heinekey, D. M.; Gould, G. L. *Organometallics* **1991**, *10*, 2977.
 (6) Pisman, P.; Snel, J. J. M. *J. Organomet. Chem.* **1984**, *276*, 387.
 (7) Foust, A. S.; Hoyano, J. K.; Graham, W. A. G. *J. Organomet. Chem.* **1971**, *32*, C65.
 (8) Casey, C. P.; Sakaba, H.; Hazin, P. N.; Powell, D. R. *J. Am. Chem. Soc.* **1991**, *113*, 8165.
 (9) Hoyano, J. K.; Graham, W. A. G. *Chem. Commun.* **1982**, 27.
 (10) Cotton, F. A.; Harris, C. B. *Inorg. Chem.* **1965**, *4*, 330–334.
 (11) Cotton, F. A.; Walton, R. A. *Multiple Bonds Between Metal Atoms*; Wiley: New York, 1982.
 (12) Radius, U.; Breher, F. *Angew. Chem., Int. Ed.* **2006**, *45*, 3006.

- (13) Ehlers, A. W.; Frenking, G. *J. Am. Chem. Soc.* **1994**, *116*, 1514.
 (14) Delley, B.; Wrinn, M.; Lüthi, H. P. *J. Chem. Phys.* **1994**, *100*, 5785.
 (15) Li, J.; Schreckenbach, G.; Ziegler, T. *J. Am. Chem. Soc.* **1995**, *117*, 486.
 (16) Jonas, V.; Thiel, W. *J. Chem. Phys.* **1995**, *102*, 8474.
 (17) Barckholtz, T. A.; Bursten, B. E. *J. Am. Chem. Soc.* **1998**, *120*, 1926.
 (18) Niu, S.; Hall, M. B. *Chem. Rev.* **2000**, *100*, 353.
 (19) Macchi, P.; Sironi, A. *Coord. Chem. Rev.* **2003**, *238*, 383.
 (20) Carreon, J.-L.; Harvey, J. N. *Phys. Chem. Chem. Phys.* **2006**, *8*, 93.
 (21) Bühl, M.; Kabrede, H. *J. Chem. Theory Comput.* **2006**, *2*, 1282.
 (22) Becke, A. D. *Phys. Rev. A* **1988**, *38*, 3098.
 (23) Perdew, J. P. *Phys. Rev. B* **1986**, *33*, 8822.
 (24) Adamo, C.; Barone, V. *J. Chem. Phys.* **1998**, *108*, 664.
 (25) Zhao, Y.; Pu, J.; Lynch, B. J.; Truhlar, D. G. *Phys. Chem. Chem. Phys.* **2004**, *6*, 673.
 (26) Perdew, J. P. In *Electronic Structure of Solids*, '91 ed.; Ziesche, P., Esching, H., Eds.; Academic Verlag: Berlin, 1991, p 11.
 (27) Feng, X.; Gu, J.; Xie, Y.; King, R. B.; Schaefer, H. F. *J. Chem. Theor. Comput.* **2007**, *3*, 1580.
 (28) Zhao, S.; Wang, W.; Li, Z.; Liu, Z. P.; Fan, K.; Xie, Y.; Schaefer, H. F. *J. Chem. Phys.* **2006**, *124*, 184102.
 (29) Andrae, D.; Haussermann, U.; Dolg, M.; Stoll, H.; Preuss, H. *Theor. Chim. Acta* **1990**, *77*, 123.
 (30) Dunning, T. H. *J. Chem. Phys.* **1970**, *53*, 2823.
 (31) Huzinaga, S. *J. Chem. Phys.* **1965**, *42*, 1293.
 (32) Frisch, M. J. et al. *Gaussian 03*, Revision C 02; Gaussian, Inc.: Wallingford, CT, 2004. (see Supporting Information for details).

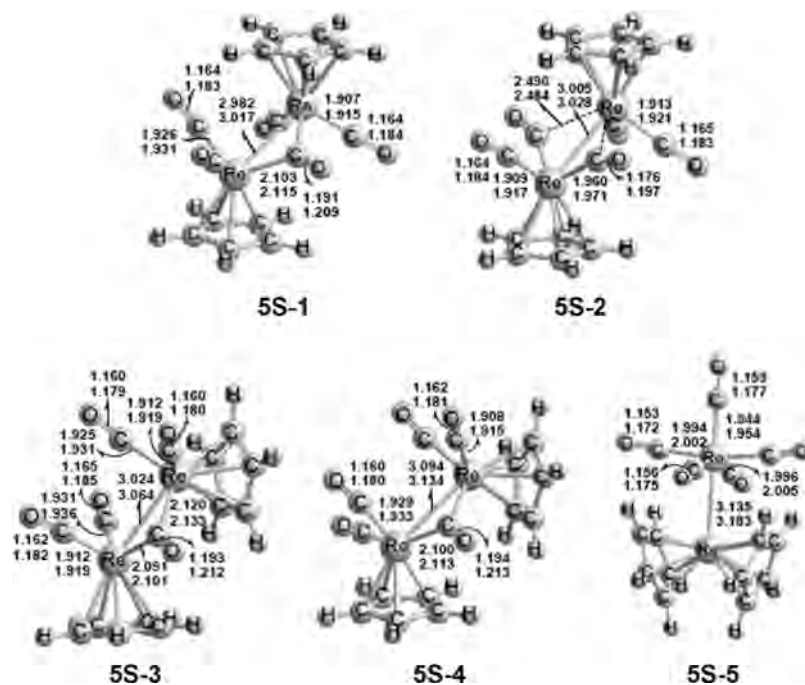


Figure 3. Structures for $\text{Cp}_2\text{Re}_2(\text{CO})_5$. The distances in Figures 3–10 are given in Å. For the bond distances listed in Figures 3–10 the upper distances were determined by the MPW1PW91 method and the lower distances by the BP86 method.

Table 1. Total Energy (E , in Hartree), Relative Energy (ΔE , in kcal/mol), Number of Imaginary Vibrational Frequencies (Nimag), and Re–Re Bond Distance (Å) for Each of the $\text{Cp}_2\text{Re}_2(\text{CO})_5$ Structures

	5S-1 (C_2)	5S-2 (C_s)	5S-3 (C_1)	5S-4 (C_s)	5S-5 (C_{2v})
	MPW1PW91				
E	–1110.55467	–1110.54326	–1110.54256	–1110.53585	–1110.48226
ΔE	0	7.2	7.6	11.8	45.4
Nimag	0	3(121i,37i,28i)	0	2(32i,25i)	0
Re–Re	2.982	3.005	3.024	3.094	3.135
	BP86				
E	–1110.99829	–1110.98793	–1110.98667	–1110.98077	–1110.92441
ΔE	0	6.5	7.3	11.0	46.4
Nimag	0	3(109i,37i,23i)	0	2(27i,23i)	1(10i)
Re–Re	3.017	3.028	3.064	3.134	3.183

was the default for evaluating integrals numerically. The finer grid (120, 974) was used for more precise resolution of the imaginary vibrational frequencies. The tight (10^{-8} hartree) designation was the default for the self-consistent field (SCF) convergence. All of the predicted triplet structures were found to have negligible spin contamination, with $\langle S^2 \rangle$ values very close to the ideal value of $S(S + 1) = 2$.

A total of 37 structures for $\text{Cp}_2\text{Re}_2(\text{CO})_n$ ($n = 5, 4, 3, 2$) derivatives were found in this research. Only those with energies within ~ 20 kcal/mol of the global minima are discussed specifically in this paper. A summary of the vibrational frequencies and geometries of these 37 structures is given in the Supporting Information.

3. Results

3.1. $\text{Cp}_2\text{Re}_2(\text{CO})_5$. The four low-lying stationary points for $\text{Cp}_2\text{Re}_2(\text{CO})_5$ (Figure 3 and Table 1) have the usual single Cp ring bonded to each metal atom (I in Figure 1). The Re–Re distances of these $\text{Cp}_2\text{Re}_2(\text{CO})_5$ structures are predicted to fall in the range 2.98–3.13 Å, consistent with

a normal Re–Re single bond.

The global minimum for $\text{Cp}_2\text{Re}_2(\text{CO})_5$ is a C_2 *trans* structure **5S-1** with one bridging carbonyl (Figure 3 and Table 1), which is very close to the experimentally determined⁷ $(\eta^5\text{-C}_5\text{H}_5)_2\text{Re}_2(\text{CO})_5$ structure. Thus, the predicted Re–Re distance in **5S-1** of 2.982 Å (MPW1PW91) or 3.017 Å (BP86) is near the experimental value of 2.957 Å and consistent with the formal Re–Re single bond giving each rhenium atom the favored 18-electron configuration. The calculated $\nu(\text{CO})$ frequencies of 1743, 1903, 1922, 1950, and 1976 cm^{-1} by the BP86 method for **5S-1** (Table 2) are remarkably close to the experimentally reported⁷ $\nu(\text{CO})$ frequencies of 1740, 1904, 1923, 1956, and 1992 cm^{-1} , respectively. The $\nu(\text{CO})$ frequency around 1740 cm^{-1} corresponds to the bridging carbonyl.

The next lowest energy $\text{Cp}_2\text{Re}_2(\text{CO})_5$ structure is a C_s structure **5S-2** with two semibridging carbonyls (Figure 3 and Table 1) lying 7.2 kcal/mol (MPW1PW91) or 6.5 kcal/mol (BP86) in energy above the global minimum **5S-1**. Three imaginary vibrational frequencies are predicted for structure **5S-2**. Following the normal mode of the largest imaginary vibrational frequency (a'') leads to **5S-1**. The calculated

(33) Blaha, J. P.; Bursten, B. E.; Dewan, J. C.; Frankel, R. B.; Randolph, C. L.; Wilson, B. A.; Wrighton, M. S. *J. Am. Chem. Soc.* **1985**, *107*, 4561.

Table 2. Infrared $\nu(\text{CO})$ Vibrational Frequencies (cm^{-1}) Predicted for the $\text{Cp}_2\text{Re}_2(\text{CO})_5$ Structures^a

	MPW1PW91	BP86
5S-1 (C_2)	1846 (a, 460), 2015 (b, 137), 2035 (a, 1534), 2065 (b, 1964), 2094 (a, 59)	1743 (a, 363), 1903 (b, 101), 1922 (a, 1287), 1950 (b, 1657), 1976 (a, 40)
expt ⁷		1740 (4.5), 1904 (1.2), 1923 (9.0), 1956 (10.0), 1992 (0.7)
5S-2 (C_s)	1940 (a'', 705), 1946 (a', 13), 2025 (a'', 1240), 2054 (a', 2051), 2085 (a', 107)	1826 (a'', 621), 1833 (a', 6), 1915 (a'', 964), 1939 (a', 1633), 1970 (a', 177)
5S-3 (C_1)	1831 (a, 495), 2017 (a, 551), 2049 (a, 688), 2066 (a, 1046), 2116 (a, 1396)	1727 (a, 391), 1904 (a, 454), 1935 (a, 633), 1950 (a, 850), 1995 (a, 1143)
5S-4 (C_s)	1825 (a', 480), 2024 (a'', 5), 2061 (a', 1720), 2069 (a'', 559), 2120 (a', 1494)	1721 (a', 373), 1911 (a'', 2), 1945 (a', 1418), 1955 (a'', 539), 1999 (a', 1204)
5S-5 (C_{2v})	2065 (a ₁ , 950), 2067 (b ₂ , 1478), 2076 (b ₁ , 1564), 2091 (a ₁ , 4), 2172(a ₁ , 620)	1943 (b ₁ , 1255), 1950 (a ₁ , 783), 1957 (b ₂ , 1308), 1967 (a ₁ , 4), 2045 (a ₁ , 577)

^a Infrared intensities in parentheses are in km/mol , bridging $\nu(\text{CO})$ frequencies are in **bold**.

$\nu(\text{CO})$ frequencies of **5S-2** at 1826 cm^{-1} and 1833 cm^{-1} (BP86, Table 2) correspond to the two semibridging CO groups in **5S-2** and are $\sim 80 \text{ cm}^{-1}$ larger than the predicted symmetrical bridging $\nu(\text{CO})$ frequency of **5S-1**.

A *cis* C_1 structure **5S-3** (Figure 3 and Table 1) of $\text{Cp}_2\text{Re}_2(\text{CO})_5$ with a single bridging CO group is also found to be a genuine minimum with all real vibrational frequencies. Structure **5S-3** lies 7.6 kcal/mol (MPW91PW91) or 7.3 kcal/mol (BP86) above the corresponding *trans* isomer and global minimum **5S-1**.

A *cis* C_s structure **5S-4** (Figure 3 and Table 1) is found to have two small imaginary vibrational frequencies. Using a finer grid (120,974) does not remove these imaginary vibrational frequencies. Following the normal mode of the largest imaginary frequency collapses **5S-4** to **5S-3**. The single essentially bridging carbonyls in structures **5S-3** and **5S-4** exhibit $\nu(\text{CO})$ frequencies at 1727 cm^{-1} and 1721 cm^{-1} (BP86, Table 2), respectively.

After structure **5S-4** for $\text{Cp}_2\text{Re}_2(\text{CO})_5$ there is a large energy gap to the next structure **5S-5** (Figure 3), which lies 46.4 kcal/mol (BP86) above the global minimum **5S-1**. Structure **5S-5** is predicted to have a small imaginary vibrational frequency at $10i$ (BP86), which is removed by using a finer integration grid (120,974). This structure, despite its high relative energy, is very interesting since it has an unusual $\text{Cp}_2\text{Re}-\text{Re}(\text{CO})_5$ structure of a type not previously found experimentally or theoretically in binuclear cyclopentadienyl metal carbonyl chemistry. Furthermore, a reaction between the known^{4,5} Cp_2ReX and $\text{NaRe}(\text{CO})_5$ might selectively lead to **5S-5** rather than to the much lower energy $\text{Cp}_2\text{Re}_2(\text{CO})_5$ structure **5S-1**.

3.2. $\text{Cp}_2\text{Re}_2(\text{CO})_4$. Five singlet (Figure 4 and Table 3) and three triplet low-lying structures (Figure 5 and Table 4) of the unsaturated $\text{Cp}_2\text{Re}_2(\text{CO})_4$ have been investigated. The global minimum found for $\text{Cp}_2\text{Re}_2(\text{CO})_4$ (**4S-1**, Figure 4) is a centrosymmetric singlet structure analogous to the known⁸ ($\eta^5\text{-Me}_5\text{C}_5$)₂ $\text{Re}_2(\text{CO})_4$, having a planar arrangement of the two semibridging carbonyls and the two rhenium atoms. The predicted $\text{Re}=\text{Re}$ distance, namely 2.711 \AA (MPW1PW91)

or 2.752 \AA (BP86), is very close to the experimental value of 2.723 \AA for the permethylated derivative ($\eta^5\text{-Me}_5\text{C}_5$)₂ $\text{Re}_2(\text{CO})_4$ and is $\sim 0.3 \text{ \AA}$ shorter than the $\text{Re}-\text{Re}$ single bonds in the structures of $\text{Cp}_2\text{Re}_2(\text{CO})_5$ (Figure 3 and Table 1). This confirms the formal $\text{Re}=\text{Re}$ double bond in **4S-1** needed to give both rhenium atoms 18-electron configurations. The $\text{Re}-\text{C}$ distances to the two semibridging CO groups in **4S-1** are 1.913 \AA and 2.464 \AA (MPW1PW91) or 1.935 \AA and 2.592 \AA (BP86), which are reasonably proximate to the experimental values⁸ of $1.921(9) \text{ \AA}$ and $2.485(9) \text{ \AA}$ for ($\eta^5\text{-Me}_5\text{C}_5$)₂ $\text{Re}_2(\text{CO})_4$. The predicted $\text{Re}-\text{C}-\text{O}$ angle, namely 167.7° (MPW1PW91) or 164.2° (BP86), is also consistent with the experimental value⁸ of $165.1(8)^\circ$. Structure **4S-1** is predicted to be a genuine minimum by BP86 method, while a $15i$ imaginary vibrational frequency is predicted by the MPW1PW91 method. This imaginary vibrational frequency decreases in magnitude to $9i$ when the finer integration grid (120,974) is used.

A C_{2h} singlet state unbridged structure **4S-2** for $\text{Cp}_2\text{Re}_2(\text{CO})_4$ (Figure 4 and Table 3) is almost degenerate in energy with **4S-1** (energy difference only $\sim 1.0 \text{ kcal/mol}$) with a small imaginary vibrational frequency at $13i$ (BP86), which increases to $18i$ when the finer grid (120, 974) is used. By following the corresponding normal mode, **4S-2** collapses to **4S-1**. The predicted $\text{Re}=\text{Re}$ distance in **4S-2**, namely, 2.575 \AA (MPW1PW91) or 2.592 \AA (BP86), is about 0.15 \AA shorter than that of **4S-1** but still can correspond to the formal $\text{Re}=\text{Re}$ double bond needed to give each rhenium atom the favored 18-electron configuration.

A singlet C_2 *cis* $\text{Cp}_2\text{Re}_2(\text{CO})_4$ structure **4S-3** with two semibridging carbonyl groups (Figure 4, Table 3) and all real vibrational frequencies lies above structure **4S-1** by 4.5 kcal/mol (MPW1PW91) or 5.2 kcal/mol (BP86). The next higher energy singlet structure for $\text{Cp}_2\text{Re}_2(\text{CO})_4$ is the *cis* doubly bridging C_s singlet structure **4S-4** with only one (negligible) imaginary vibrational frequency at $3i$ (BP86), which is removed by the finer integration grid (120, 974). Structure **4S-4** is predicted to lie above **4S-1** in energy by 10.8 kcal/mol (MPW1PW91) or 6.9 kcal/mol (BP86). The $\text{Re}=\text{Re}$ distances in the range 2.7 to 2.8 \AA predicted for both structures **4S-3** and **4S-4** are consistent with the formal double bonds required to give both rhenium atoms the favored 18-electron configurations.

The next higher singlet structure for $\text{Cp}_2\text{Re}_2(\text{CO})_4$ is a $\text{Cp}_2\text{Re}-\text{Re}(\text{CO})_4$ structure **4S-5** (Figure 4 and Table 3) with two Cp rings bonded to one rhenium atom and only carbonyl groups bonded to the second rhenium atom (**III** in Figure 1). This structure lies 12.0 kcal/mol (MPW1PW91) or 15.2 kcal/mol (BP86) above the global minimum **4S-1** and has all real vibrational frequencies. Structure **4S-5** can be derived from $\text{Cp}_2\text{Re}-\text{Re}(\text{CO})_5$ (**5S-5** in Figure 3) by removal of one carbonyl group. The distance between the top rhenium atom and the hydrogen atom on the top of the left Cp ring in **4S-5** is predicted to be very short, namely 2.068 \AA (MPW1PW91) or 2.099 \AA (BP86). Furthermore, the $\text{C}-\text{H}$ bond distance is predicted to be $\sim 0.04 \text{ \AA}$ longer than the normal $\text{C}-\text{H}$ bond length suggesting a $\text{C}-\text{H}-\text{Re}$ three-center two-electron agostic bond. The distance between the two rhenium atoms

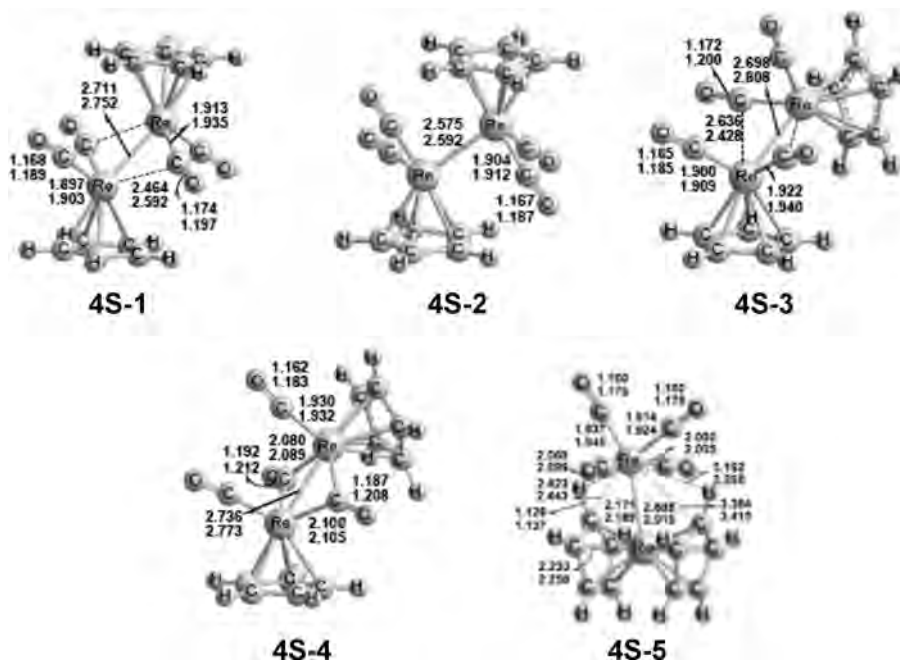


Figure 4. Singlet state structures for $\text{Cp}_2\text{Re}_2(\text{CO})_4$.

Table 3. Total Energy (E , in Hartree), Relative Energy (ΔE , in kcal/mol), Number of Imaginary Vibrational Frequencies (Nimag), and Re–Re Bond Distance (\AA) for Each of the Singlet $\text{Cp}_2\text{Re}_2(\text{CO})_4$ Structures.

	4S-1 (C_i)	4S-2 (C_{2h})	4S-3 (C_2)	4S-4 (C_s)	4S-5 (C_s)
	MPW1PW91				
E	−997.17316	−997.17145	−997.16591	−997.15587	−997.15406
ΔE	0	1.1	4.5	10.8	12.0
Nimag	1 (15i)	1 (48i)	0	1 (22i)	0
Re–Re	2.711	2.575	2.698	2.736	2.888
	BP86				
E	−997.58556	−997.58636	−997.57723	−997.57454	−997.56131
ΔE	0	−0.5	5.2	6.9	15.2
Nimag	0	1 (13i)	0	1 (3i)	0
Re–Re	2.752	2.592	2.808	2.773	2.919

Table 4. Total Energy (E , in Hartree), Relative Energy (ΔE , in kcal/mol), Number of Imaginary Vibrational Frequencies (Nimag), Re–Re Bond Distance (\AA), and Spin Contamination ($\langle S^2 \rangle$) for Each of the Triplet $\text{Cp}_2\text{Re}_2(\text{CO})_4$ Structures.

	4T-1 (C_{2h})	4T-2 (C_{2h})	4T-3 (C_{2v})
	MPW1PW91		
E	−997.15840	−997.15582	−997.15408
ΔE	9.3	10.9	12.0
Nimag	0	0	0
Re–Re	2.658	2.677	2.673
$\langle S^2 \rangle$	2.02	2.03	2.02
	BP86		
E	−997.57284	−997.56806	−997.56881
ΔE	8.0	11.0	10.5
Nimag	0	0	0
Re–Re	2.682	2.638	2.703
$\langle S^2 \rangle$	2.00	2.00	2.00

in **4S-5** is predicted to be $\sim 0.25 \text{ \AA}$ shorter than that of **5S-5** in accord with the formal $\text{Re}=\text{Re}$ double bond required to give both rhenium atoms the favored 18-electron configuration in a formally dipolar structure $\text{Cp}_2\text{Re}^+=\text{Re}^-(\text{CO})_4$.

The three triplet structures **4T-1** (C_{2h}), **4T-2** (C_{2h}) and **4T-3** (C_{2v}) (Figure 5, Table 4) were found to be almost degenerate in energy within ~ 3 kcal/mol and to lie above the global minimum **4S-1** by ~ 10 kcal/mol. The $\text{Re}=\text{Re}$ bond distances in these three structures are predicted to fall in the range of

2.64 to 2.70 \AA corresponding to double bonds, possibly of the $\sigma +^2/2\pi$ type with two unpaired electrons, similar to the double bonds in dioxygen and $\text{Cp}_2\text{Fe}_2(\mu\text{-CO})_3$ (ref 33). All three of these triplet structures are predicted to be genuine minima with all real vibrational frequencies. Structures **4T-1** (C_{2h}) and **4T-3** (C_{2v}) are *trans* and *cis* doubly CO-bridged structures, respectively, whereas structure **4T-2** (C_{2h}) is a unbridged structure.

Table 5 summarizes the $\nu(\text{CO})$ vibrational frequencies predicted for the $\text{Cp}_2\text{Re}_2(\text{CO})_4$ structures. The $\nu(\text{CO})$ frequencies in the range 1817–1845 cm^{-1} correspond to semibridging carbonyl groups, while the lower fundamentals from 1731 cm^{-1} to 1756 cm^{-1} correspond to bridging carbonyl groups. The predicted two strong infrared $\nu(\text{CO})$ frequencies for **4S-1** of 1845 and 1908 cm^{-1} (BP86) correspond fairly closely to the experimental values⁸ of 1809 and 1860 cm^{-1} for $(\eta^5\text{-Me}_5\text{C}_5)_2\text{Re}_2(\text{CO})_4$, when the effect of complete methyl substitution in lowering $\nu(\text{CO})$ frequencies is considered.

3.3. $\text{Cp}_2\text{Re}_2(\text{CO})_3$. The global minimum predicted for $\text{Cp}_2\text{Re}_2(\text{CO})_3$ is a singlet C_{2v} structure **3S-1** (Figure 6 and Table 6) with three equivalent bridging carbonyl groups. No other structures for $\text{Cp}_2\text{Re}_2(\text{CO})_3$ were found within 18 kcal/



Figure 5. Triplet state structures for $\text{Cp}_2\text{Re}_2(\text{CO})_4$.

Table 5. Infrared $\nu(\text{CO})$ Vibrational Frequencies (cm^{-1}) Predicted for $\text{Cp}_2\text{Re}_2(\text{CO})_4$ ^a

	MPW1PW91	BP86
4S-1 (C_i)	1968 ($a_g, 0$), 1980 ($a_u, 1537$), 2027 ($a_u, 1999$), 2049 ($a_g, 0$)	1833 ($a_g, 0$), 1845 ($a_u, 1037$), 1908 ($a_u, 1736$), 1927 ($a_g, 0$)
4S-2 (C_{2h})	1980 ($b_g, 0$), 2008 ($a_u, 1797$), 2044 ($b_u, 2132$), 2080 ($a_g, 0$)	1874 ($b_g, 0, 0$), 1896 ($a_u, 1517$), 1935 ($b_u, 1627$), 1962 ($a_g, 0$)
4S-3 (C_2)	1980 ($a, 84$), 1998 ($b, 1491$), 2028 ($b, 490$), 2082 ($a, 1651$)	1817 ($a, 82$), 1830 ($b, 926$), 1908 ($b, 351$), 1949 ($a, 1400$)
4S-4 (C_s)	1837 ($a', 664$), 1876 ($a', 848$), 2022 ($a'', 440$), 2081 ($a', 1587$)	1732 ($a', 4733$), 1756 ($a', 618$), 1901 ($a'', 452$), 1950 ($a', 1333$)
4S-5 (C_s)	2050 ($a', 1126$), 2075 ($a', 713$), 2080 ($a'', 1590$), 2163 ($a', 526$)	1938 ($a', 984$), 1951 ($a'', 1364$), 1956 ($a', 495$), 2033 ($a', 510$)
4T-1 (C_{2h})	1866 ($a_u, 1315$), 1872 ($a_g, 0$), 2029 ($b_u, 2217$), 2051 ($a_g, 0$)	1745 ($a_u, 0$), 1748 ($a_u, 940$), 1911 ($b_u, 1822$), 1929 ($a_g, 0$)
4T-2 (C_{2h})	1999 ($b_g, 0$), 2011 ($a_u, 2025$), 2024 ($b_u, 1878$), 2073 ($a_g, 0$)	1892 ($b_g, 0$), 1895 ($a_u, 1743$), 1917 ($b_u, 1712$), 1954 ($a_g, 0$)
4T-3 (C_{2v})	1851 ($b_1, 1264$), 1856 ($a_1, 82$), 2027 ($b_2, 511$), 2082 ($a_1, 1632$)	1731 ($b_1, 915$), 1731 ($a_1, 62$), 1909 ($b_2, 438$), 1955 ($a_1, 1321$)

^a Infrared intensities in parentheses are in km/mol , bridging and semibridging $\nu(\text{CO})$ frequencies are in **bold**.

mol of this global minimum, indicating that **3S-1** is a highly favored structure for $\text{Cp}_2\text{Re}_2(\text{CO})_3$. The two small imaginary vibrational frequencies at 29i and 27i in **3S-1** correspond to rotation of the two Cp rings and decrease to 4i and 3i if the finer integration grid (120, 974) is used. The $\text{Re}\equiv\text{Re}$ bond distance in **3S-1** of 2.427 Å (MPW1PW91) or 2.451 Å (BP86) is ~ 0.3 Å shorter than that in **4S-1** consistent with the formal triple bond required to give both rhenium atoms the favored 18-electron configuration. Furthermore, this $\text{Re}\equiv\text{Re}$ distance is very close to the 2.411 Å $\text{Re}\equiv\text{Re}$ distance found by X-ray diffraction⁹ in the closely related permethyl derivative ($\eta^5\text{-Me}_5\text{C}_5$) $_2\text{Re}_2(\mu\text{-CO})_3$. The two highly infrared-active calculated $\nu(\text{CO})$ frequencies of 1777 and 1779 cm^{-1} for **3S-1** are consistent with the experimental observation of a single $\nu(\text{CO})$ frequency at 1748 cm^{-1} in the permethylated derivative ($\eta^5\text{-Me}_5\text{C}_5$) $_2\text{Re}_2(\mu\text{-CO})_3$ after considering the $\nu(\text{CO})$ frequency lowering effects of the methyl substituents and the experimental problems of resolving two $\nu(\text{CO})$ frequencies separated by only 2 cm^{-1} .

Another singlet structure **3S-3** (C_1) for $\text{Cp}_2\text{Re}_2(\text{CO})_3$ (Figure 6, Table 6) with two bridging carbonyls is found to be a genuine minimum, lying 25.1 kcal/mol (MPW1PW91) or 28.0 kcal/mol above the global minimum **3S-1**. The

predicted $\text{Re}\text{--}\text{Re}$ distance of 2.507 Å (MPW1PW91) or 2.491 Å (BP86) in **3S-3** is representative of a $\text{Re}\equiv\text{Re}$ triple bond. Two semibridging CO groups and one terminal CO group are predicted for **3S-3** by the MPW1PW91 method. However, the BP86 method predicts one bridging, one semibridging, and one terminal carbonyl group for **3S-3**. These BP86 results are consistent with the predicted $\nu(\text{CO})$ frequencies (Table 7). For example, the predicted $\nu(\text{CO})$ frequencies of 1795 cm^{-1} , 1846 cm^{-1} , and 1963 cm^{-1} for the BP86 structure **3S-3** correspond to the bridging, semibridging, and terminal CO groups, respectively.

Structure **3S-2** for $\text{Cp}_2\text{Re}_2(\text{CO})_3$ (Figure 6, Table 6) is a $\text{Cp}_2\text{Re}\text{--}\text{Re}(\text{CO})_3$ structure (**III** in Figure 1), which is predicted to lie 18.0 kcal/mol (MPW1PW91) or 23.6 kcal/mol (BP86) above structure **3S-1**. Structure **3S-2**, which is a genuine minimum with all real vibrational frequencies, can be derived from **4S-5** (Figure 4) by removal of one of the CO groups. One of the Cp hydrogens in **3S-2** appears to be an agostic hydrogen bridging a ring carbon atom to the rhenium atom bearing the carbonyl groups as indicated by a predicted $\text{Re}\text{--}\text{H}$ distance of 2.560 Å (MPW1PW91) or 2.553 Å (BP86). The 3087 cm^{-1} (BP86) $\nu(\text{C}\text{--}\text{H})$ vibrational frequency involving this agostic hydrogen is 80 cm^{-1} lower than the other $\nu(\text{C}\text{--}\text{H})$ vibrational frequencies consistent with a weaker $\text{C}\text{--}\text{H}$ bond and the longer predicted $\text{C}\text{--}\text{H}$ bond distance.

Triplet structures for $\text{Cp}_2\text{Re}_2(\text{CO})_3$ are not considered here since the lowest lying triplet structure was found to lie more than 30 kcal/mol above the global minimum **3S-1**.

3.4. $\text{Cp}_2\text{Re}_2(\text{CO})_2$. Seven structures (four singlet and three triplet) for $\text{Cp}_2\text{Re}_2(\text{CO})_2$ were found within 30 kcal/mol of the global minimum (Figures 7 and 8 and Tables 8–10). The global minimum found for $\text{Cp}_2\text{Re}_2(\text{CO})_2$ can be either a triplet **2T-1** (C_{2v}) or a singlet **2S-1** (C_1) depending on the method. Thus, the MPW1PW91 method predicts the triplet **2T-1** to be the global minimum with the singlet **2S-1** lying 2.9 kcal/mol higher in energy than **2T-1**. However, the BP86 method predicts the singlet structure **2S-1** to lie below **2T-1** by 4.3 kcal/mol.

The lowest energy structures **2S-1** and **2T-1** for $\text{Cp}_2\text{Re}_2(\text{CO})_2$ are both doubly bridging structures having all real vibrational frequencies. The $\text{Re}\equiv\text{Re}$ distance of 2.466 Å (MPW1PW91) or 2.490 Å (BP86) in the triplet **2T-1** lies within the 2.43 Å to 2.51 Å range found for the $\text{Re}\equiv\text{Re}$ formal triple bonds in the $\text{Cp}_2\text{Re}_2(\text{CO})_3$ isomers **3S-1** and **3T-3**. This suggests the formal triple bond in **2T-1** required

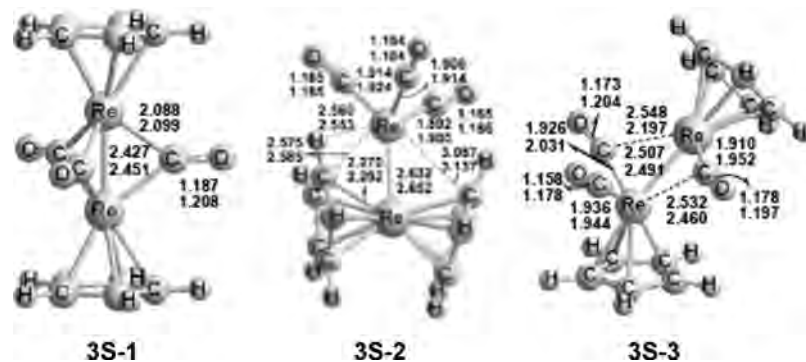


Figure 6. Structures for $\text{Cp}_2\text{Re}_2(\text{CO})_3$ within 30 kcal/mol of the global minimum **3S-1**.

Table 6. Total Energy (E , in Hartree), Relative Energy (ΔE , in kcal/mol), Number of Imaginary Vibrational Frequencies (Nimag), and Re–Re Bond Distance (Å) for Each of the $\text{Cp}_2\text{Re}_2(\text{CO})_3$ Structures

	3S-1 (C_{2v})	3S-2 (C_1)	3S-3 (C_1)
MPW1PW91			
E	−883.84193	−883.81325	−883.80191
ΔE	0	18.0	25.1
Nimag	2(29i,27i)	0	0
Re–Re	2.427	2.632	2.507
BP86			
E	−884.223978	−884.18633	−884.17930
ΔE	0	23.6	28.0
Nimag	2(29i,27i)	0	0
Re–Re	2.451	2.652	2.491

Table 7. Infrared $\nu(\text{CO})$ Vibrational Frequencies (cm^{-1}) Predicted for the $\text{Cp}_2\text{Re}_2(\text{CO})_3$ Structures^a

	MPW1PW91	BP86
3S-1 (C_{2v})	1890 (b ₁ , 1327), 1892 (a ₁ , 1348), 1918 (a ₁ , 2)	1777 (b ₁ , 1023), 1779 (a ₁ , 1036), 1805 (a ₁ , 1)
3S-2 (C_1)	2018 (a, 1141), 2023 (a, 1273), 2113 (a, 926)	1904 (a, 952), 1909 (a, 1036), 1989 (a, 707)
3S-3 (C_1)	1961 (a, 590), 1991 (a, 929), 2092 (a, 1109)	1795 (a, 594), 1846 (a, 547), 1963 (a, 1021)

^a Infrared intensities in parentheses are in km/mol, bridging $\nu(\text{CO})$ frequencies are in **bold**.

to give both rhenium atoms the 17-electron configurations needed for triplet spin multiplicity. The ReRe distance in the singlet **2S-1** of 2.395 Å (MPW1PW91) or 2.396 Å (BP86) is significantly shorter than the $\text{Re}\equiv\text{Re}$ distance in the triplet **2T-1**. This appears consistent with the formal metal–metal quadruple bond needed to give both rhenium atoms in **2S-1** the favored 18-electron configuration. The $\nu(\text{CO})$ frequencies of 1759 and 1768 cm^{-1} for **2S-1**, as well as 1746 and 1754 cm^{-1} for **2T-1** (Table 10), are consistent with symmetrical bridging carbonyl groups.

Another doubly bridged singlet structure **2S-2** for $\text{Cp}_2\text{Re}_2(\text{CO})_2$ (Figure 7 and Table 8) is predicted to lie within ~0.6 kcal/mol in energy of **2S-1**. Structure **2S-2** is predicted to have a single imaginary vibrational frequency at 31i cm^{-1} (BP86) or two imaginary vibrational frequencies at 79i cm^{-1} and 31i cm^{-1} (MPW1PW91). Using a finer integration grid (120, 974) reduces the imaginary frequencies to 13i cm^{-1} and 3i cm^{-1} (BP86). The ReRe distance in **2S-2** is essentially identical to that in **2S-1** consistent with a similar formal quadruple bond.

The triplet structure **2T-2** (Figure 8 and Table 9) with two semibridging CO groups is predicted to be a genuine minimum, lying 4.1 kcal/mol (MPW1PW91) or 4.8 kcal/

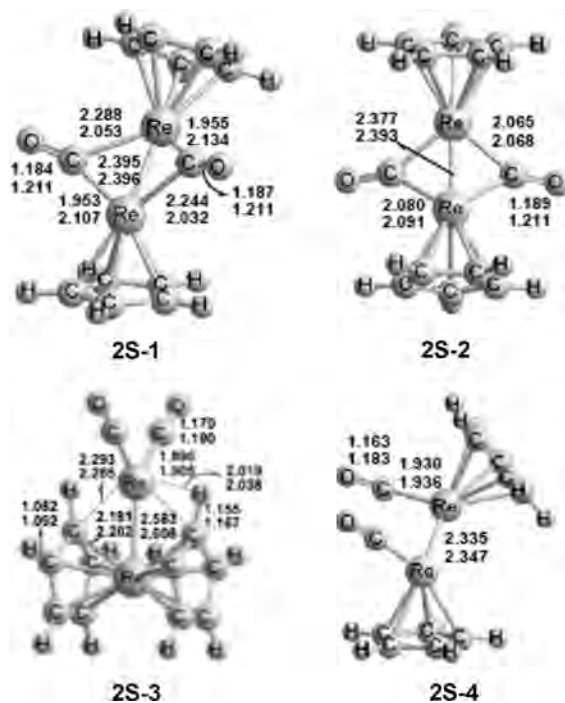


Figure 7. Singlet structures for $\text{Cp}_2\text{Re}_2(\text{CO})_2$.

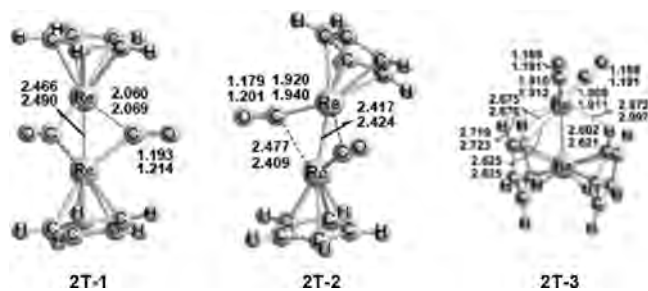


Figure 8. Triplet structures for $\text{Cp}_2\text{Re}_2(\text{CO})_2$.

mol (BP86) higher in energy than **2T-1**. The $\text{Re}\equiv\text{Re}$ distance in **2T-2** is predicted to be 2.417 Å (MPW1PW91) or 2.424 Å (BP86), which corresponds to the formal triple bond required to give both rhenium atoms 17-electron configurations for the triplet electronic state. The $\nu(\text{CO})$ frequencies at 1823 and 1832 cm^{-1} (BP86, Table 10) correspond to the two semibridging carbonyl groups of **2T-2**.

A triplet $\text{Cp}_2\text{Re}-\text{Re}(\text{CO})_2$ structure **2T-3** (C_1) is predicted to lie 15.2 kcal/mol (MPW1PW91) or 18.5 kcal/mol (BP86) in energy above **2T-1** (Figure 8, Table 9) with all real vibrational frequencies. The $\text{Re}\equiv\text{Re}$ bond distance of 2.602

Table 8. Total Energy (E , in Hartree), Relative Energy (ΔE , in kcal/mol), Number of Imaginary Vibrational Frequencies (Nimag), and Re–Re Bond Distance (\AA) for Each of the Singlet $\text{Cp}_2\text{Re}_2(\text{CO})_2$ Structures

	2S-1 (C_1)	2S-2 (C_s)	2S-3 (C_{2v})	2S-4 (C_2)
MPW1PW91				
E	-770.41335	-770.41247	-770.40730	-770.37669
ΔE	2.9	3.5	6.7	25.9
Nimag	0	2(79i, 31i)	0	0
Re–Re	2.395	2.377	2.583	2.335
BP86				
E	-770.76647	-770.76635	-770.74915	-770.73418
ΔE	-4.3	-4.3	6.5	15.9
Nimag	0	1(31i)	0	0
Re–Re	2.396	2.393	2.608	2.347

Table 9. Total Energy (E , in Hartree), Relative Energy (ΔE , in kcal/mol), Number of Imaginary Vibrational Frequencies (Nimag), Re–Re Bond Distance (\AA), and Spin Contamination ($\langle S^2 \rangle$) for Each of the Triplet $\text{Cp}_2\text{Re}_2(\text{CO})_2$ Structures.

	2T-1 (C_{2v})	2T-2 (C_2)	2T-3 (C_1)
MPW1PW91			
E	-770.41804	-770.41153	-770.39380
ΔE	0	4.1	15.2
Nimag	0	0	0
Re–Re	2.466	2.417	2.602
$\langle S^2 \rangle$	2.02	2.01	2.01
BP86			
E	-770.75957	-770.75195	-770.73003
ΔE	0	4.8	18.5
Nimag	0	0	0
Re–Re	2.490	2.424	2.621
$\langle S^2 \rangle$	2.01	2.01	2.01

Table 10. Infrared $\nu(\text{CO})$ Vibrational Frequencies (cm^{-1}) Predicted For $\text{Cp}_2\text{Re}_2(\text{CO})_2$ ^a

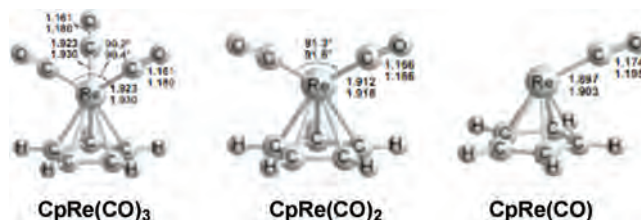
	MPW1PW91	BP86
2S-1 (C_1)	1899 (a, 1017), 1920 (a, 654)	1759 (a, 1096), 1768 (a, 180)
2S-2 (C_s)	1873 (a'', 1468), 1883 (a', 237)	1756 (a'', 1105), 1766 (a', 178)
2S-3 (C_{2v})	1990 (b ₂ , 1363), 2049 (a ₁ , 1345)	1877 (b ₂ , 1127), 1928 (a ₁ , 1054)
2S-4 (C_2)	2020 (b, 641), 2074 (a, 1444)	1907 (b, 515), 1950 (a, 1150)
2T-1 (C_{2v})	1856 (b₁, 1454), 1865 (a₁, 181)	1746 (b₁, 1102), 1754 (a₁, 124)
2T-2 (C_2)	1951 (b, 1488), 1964 (a, 291)	1823 (b, 1107), 1832 (a, 215)
2T-3 (C_1)	1957 (a, 1893), 2042 (a, 1220)	1845 (a, 1380), 1913 (a, 923)

^a Infrared intensities in parentheses are in km/mol, bridging $\nu(\text{CO})$ frequencies are in **bold**.

\AA (MPW1PW91) or 2.621 \AA (BP86) may be interpreted as a long triple bond required to give both rhenium atoms the 17-electron configuration for the triplet electronic state.

A $\text{Cp}_2\text{Re}-\text{Re}(\text{CO})_2$ singlet structure with all real vibrational frequencies is also found for $\text{Cp}_2\text{Re}_2(\text{CO})_2$, namely the C_{2v} structure **2S-3** at 6.7 kcal/mol (MPW1PW91) or 6.5 kcal/mol (BP86) above **2T-1** (Figure 7, Table 8). Structure **2S-3** has an agostic hydrogen atom bridging from each Cp ring to the highly unsaturated $\text{Re}(\text{CO})_2$ unit with a Re–H distance of 2.019 \AA (MPW1PW91) or 2.038 \AA (BP86). The $\nu(\text{CO})$ frequencies in **2S-3** are predicted to be 1877 and 1928 cm^{-1} (BP86), consistent with only terminal CO groups.

The only unbridged $\text{Cp}_2\text{Re}_2(\text{CO})_2$ singlet structure **2S-4** (Figure 7 and Table 8) is predicted to lie in energy above

**Figure 9.** Optimized mononuclear $\text{CpRe}(\text{CO})_m$ ($m = 3, 2, 1$) fragments used to calculate dissociation energies.

2T-1 by 25.9 kcal/mol (MPW1PW91) or 15.9 kcal/mol (BP86) with all real vibrational frequencies. The ReRe distance in **2S-4** is found to be the shortest for all of the $\text{Cp}_2\text{Re}_2(\text{CO})_2$ structures, namely 2.335 \AA (MPW1PW91) or 2.347 \AA (BP86) corresponding to the formal quadruple bond required to give each rhenium atom the favored 18-electron configuration. The $\nu(\text{CO})$ frequencies for **2S-4** are predicted to be 1907 and 1950 cm^{-1} (Table 10) consistent with terminal carbonyl groups.

3.5. $\text{CpRe}(\text{CO})_m$, $\text{Re}(\text{CO})_n$ and Cp_2Re Fragments. To determine the energies of dissociation of $\text{Cp}_2\text{Re}_2(\text{CO})_n$ derivatives into two mononuclear $\text{CpRe}(\text{CO})_m$ fragments or $\text{Cp}_2\text{Re} + \text{Re}(\text{CO})_n$ fragments, the mononuclear $\text{CpRe}(\text{CO})_m$ and $\text{Re}(\text{CO})_n$ derivatives were also investigated using the same DFT methods. The optimized structures and total energies of the $\text{CpRe}(\text{CO})_m$ ($m = 3, 2, 1$) structures are shown in Figure 9 and Table 11, respectively. Of interest is the fact that the lone carbonyl group in $\text{CpRe}(\text{CO})$ is bent away from the C_5 axis of the Cp ring. This $\text{CpRe}(\text{CO})$ structure arises by loss of one CO group from the optimized $\text{CpRe}(\text{CO})_2$ structure, with relatively little rearrangement after CO loss (Figure 9).

The optimized structures, total energies, and spin contamination ($\langle S^2 \rangle$) for $\text{Re}(\text{CO})_n$ ($n = 5, 4, 3, 2, 1$) and Cp_2Re are shown in Figure 10 and Table 12. The lowest energy structures for $\text{Re}(\text{CO})_5$, $\text{Re}(\text{CO})_4$, $\text{Re}(\text{CO})_3$, $\text{Re}(\text{CO})_2$, and $\text{Re}(\text{CO})$ are the doublet C_{4v} square pyramid (half of $\text{Re}_2(\text{CO})_{10}$), doublet D_{4h} square planar, quartet C_{3v} pyramidal, doublet bent C_{2v} , and quartet $C_{\infty v}$ linear, respectively (Figure 10). The lowest energy structure for Cp_2Re is a doublet D_{5h} eclipsed sandwich structure. The $\langle S^2 \rangle$ values for the doublet and quartet structures in Figure 10 are very close to the ideal $S(S + 1)$ values of 0.75 and 3.75, respectively, indicating no significant spin contamination in any of these structures.

3.6. Dissociation and Disproportionation Reactions. The bond dissociation energy (BDE) for the loss of one carbonyl group from $\text{Cp}_2\text{Re}_2(\text{CO})_4$ to give $\text{Cp}_2\text{Re}_2(\text{CO})_3$ is 20.0 kcal/mol (MPW1PW91) or 18.3 kcal/mol (BP86), which is much smaller than the BDEs for carbonyl loss from either $\text{Cp}_2\text{Re}_2(\text{CO})_5$ or $\text{Cp}_2\text{Re}_2(\text{CO})_3$ (Table 13). Furthermore, the BDEs for $\text{Cp}_2\text{Re}_2(\text{CO})_5$ and $\text{Cp}_2\text{Re}_2(\text{CO})_3$ (Table 13) are seen to be much larger than the BDEs of 27 kcal/mol, 41 kcal/mol, and 37 kcal/mol reported³⁴ for $\text{Ni}(\text{CO})_4$, $\text{Fe}(\text{CO})_5$, and $\text{Cr}(\text{CO})_6$, respectively.

The reaction energies for the disproportionations $2\text{Cp}_2\text{Re}_2(\text{CO})_n \rightarrow \text{Cp}_2\text{Re}_2(\text{CO})_{n+1} + \text{Cp}_2\text{Re}_2(\text{CO})_{n-1}$ (Table

(34) Sunderlin, L. S.; Wang, D. N.; Squires, R. R. *J. Am. Chem. Soc.* **1993**, *115*, 12060.

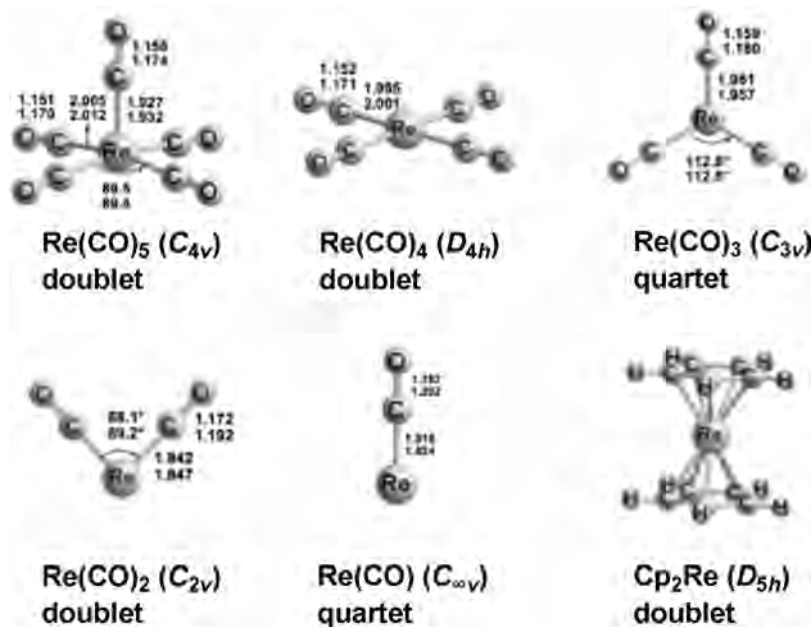


Figure 10. Optimized structures for the $\text{Re}(\text{CO})_n$ ($n = 5, 4, 3, 2, 1$) and Cp_2Re fragments.

Table 11. Total Energies (E , in Hartree) and Number of Imaginary Vibrational Frequencies (Nimag) for the Global Minima Of $\text{CpRe}(\text{CO})_m$

	$\text{CpRe}(\text{CO})_3$ (C_s)	$\text{CpRe}(\text{CO})_2$ (C_s)	$\text{CpRe}(\text{CO})$ (C_s)
MPW1PW91			
E	-611.95791	-498.54373	-385.13212
Nimag	0	0	0
BP86			
E	-612.19747	-498.74955	-385.30189
Nimag	0	0	0

14) suggest that $\text{Cp}_2\text{Re}_2(\text{CO})_4$ is likely to be a thermodynamically unstable molecule owing to exothermic disproportionation, as well as its relatively low CO dissociation energy (Table 13). However, $\text{Cp}_2\text{Re}_2(\text{CO})_3$ is stable with respect to similar disproportionation.

The dissociation of $\text{Cp}_2\text{Re}_2(\text{CO})_n$ into mononuclear fragments can occur in two ways. The first is the dissociation of $\text{Cp}_2\text{Re}_2(\text{CO})_n$ into the fragments $\text{CpRe}(\text{CO})_p + \text{CpRe}(\text{CO})_q$ where $p + q = n$ and each fragment has a cyclopentadienyl ring bonded to the rhenium atom. Table 15 lists these dissociation energies for the lowest energy $\text{Cp}_2\text{Re}_2(\text{CO})_n$ structures, which are all seen to be highly endothermic. The lowest of these dissociation energies is 33.3 kcal/mol (MPW1PW91) or 31.2 kcal/mol (BP86) for the dissociation of $\text{Cp}_2\text{Re}_2(\text{CO})_5$ into $\text{CpRe}(\text{CO})_3$ and $\text{CpRe}(\text{CO})_2$. All of the other dissociation energies for reactions of this type are more than 50 kcal/mol. These results indicate the strength of the rhenium–rhenium bonding in these binuclear systems.

A new feature of the binuclear cyclopentadienylrhenium carbonyl chemistry encountered in this work is the existence of derivatives with structures of the type $\text{Cp}_2\text{Re}-\text{Re}(\text{CO})_n$ (**III** in Figure 1) in which the two Cp rings are bonded to the same rhenium atom and the other rhenium atom bears only carbonyl groups. Table 16 summarizes the dissociation energies of the lowest lying such structures into $\text{Cp}_2\text{Re} + \text{Re}(\text{CO})_n$ fragments. These processes are seen to be highly unfavorable, requiring energies in excess of 70 kcal/mol in

every case. This again indicates strong rhenium–rhenium bonding.

4. Discussion

4.1. $\text{Cp}_2\text{Re}-\text{Re}(\text{CO})_n$ Derivatives and Agostic Hydrogen Atoms. Our studies on binuclear cyclopentadienyl metal carbonyl derivatives $\text{Cp}_2\text{M}_2(\text{CO})_n$ of the first row transition metals ($\text{M} = \text{V},^{35} \text{Cr},^{36} \text{Mn},^{37} \text{Fe},^1 \text{Co},^2 \text{Ni}^3$) have not led to any structures of the type $\text{Cp}_2\text{M}-\text{M}(\text{CO})_n$, with both cyclopentadienyl rings bonded to a single metal atom and the other metal atom bearing only carbonyl groups (**III** in Figure 1). However, we find such compounds for rhenium (Table 17). The simplest such compound is $\text{Cp}_2\text{Re}-\text{Re}(\text{CO})_5$ (**5S-5** in Figure 3). The structure for this compound can be derived from the well-known Cp_2ReH by replacement of the hydride with a $\text{Re}(\text{CO})_5$ group. The single Re–Re bond distance in $\text{Cp}_2\text{Re}-\text{Re}(\text{CO})_5$ (**5S-5**) at 3.135 Å (MPW1PW91) or 3.183 Å (BP86) is significantly longer than the Re–Re single bond of 3.041 Å found by X-ray diffraction³⁸ in $\text{Re}_2(\text{CO})_{10}$.

The Re–Re distance decreases from 3.183 Å (BP86) in $\text{Cp}_2\text{Re}-\text{Re}(\text{CO})_5$ to 2.919 Å (BP86) in $\text{Cp}_2\text{Re}-\text{Re}(\text{CO})_4$, (**4S-5**). This comparison is consistent with formation of a dipolar $\text{Re}=\text{Re}$ double bond leading to a formal structure $\text{Cp}_2\text{Re}^+=\text{Re}^-(\text{CO})_4$ giving both rhenium atoms the favored 18-electron configuration. One of the Cp hydrogens becomes an agostic hydrogen forming a C–H–Re bridge as recognized by a relatively short Re–H distance of 2.099 Å (BP86). Such agostic hydrogen atoms forming C–H–M bridges to

(35) Li, Q.; Zhang, X.; Xie, Y.; King, R. B.; Schaefer, H. F. *J. Am. Chem. Soc.* **2007**, *129*, 3433.

(36) Fortman, G. C.; Kégl, T.; Li, Q.-S.; Zhang, X.; Schaefer, H. F.; Xie, Y.; King, R. B.; Telser, J.; Hoff, C. D. *J. Am. Chem. Soc.* **2007**, *129*, 14388.

(37) Zhang, X.; Li, Q.-S.; Xie, Y.; King, R. B.; Schaefer, H. F. *Organometallics* **2008**, *27*, 61.

(38) Churchill, M. R.; Amoh, K. N.; Wasserman, H. J. *Inorg. Chem.* **1981**, *20*, 1609.

Table 12. Total Energies (E , in Hartree), Spin Contaminations ($\langle S^2 \rangle$), and Numbers of Imaginary Vibrational Frequencies (Nimag) for the Global Minima of $\text{Re}(\text{CO})_n$ and Cp_2Re

	$\text{Re}(\text{CO})_5$ doublet (C_{4v})	$\text{Re}(\text{CO})_4$ doublet (D_{4h})	$\text{Re}(\text{CO})_3$ quartet (C_{3v})	$\text{Re}(\text{CO})_2$ doublet (C_{2v})	$\text{Re}(\text{CO})$ quartet ($C_{\infty v}$)	Cp_2Re doublet (D_{5h})
MPW1PW91						
E	-645.35073	-531.68322	-418.26984	-304.93112	-191.55356	-465.37505
Nimag	0	0	0	0	0	0
$\langle S^2 \rangle$	0.75	0.76	3.76	0.76	3.80	0.76
BP86						
E	-645.06904	-531.93109	-418.48153	-305.10628	-191.67953	-465.53260
Nimag	0	0	0	0	0	0
$\langle S^2 \rangle$	0.75	0.76	3.76	0.76	3.80	0.76

Table 13. Dissociation Energies (kcal/mol) for the Successive Removal of Carbonyl Groups from the $\text{Cp}_2\text{Re}_2(\text{CO})_n$ Derivatives

process	MPW1PW91	BP86
$\text{Cp}_2\text{Re}_2(\text{CO})_5$ (5S-1) \rightarrow $\text{Cp}_2\text{Re}_2(\text{CO})_4$ (4S-1) + CO	51.7	50.5
$\text{Cp}_2\text{Re}_2(\text{CO})_4$ (4S-1) \rightarrow $\text{Cp}_2\text{Re}_2(\text{CO})_3$ (3S-1) + CO	20.0	18.3
$\text{Cp}_2\text{Re}_2(\text{CO})_3$ (3S-1) \rightarrow $\text{Cp}_2\text{Re}_2(\text{CO})_2$ (2T-1) + CO	78.3	83.1

Table 14. Disproportionation Energies (kcal/mol)

	MPW1PW91	BP86
$2\text{Cp}_2\text{Re}_2(\text{CO})_4 \rightarrow \text{Cp}_2\text{Re}_2(\text{CO})_5 + \text{Cp}_2\text{Re}_2(\text{CO})_3$	-31.7	-32.2
$2\text{Cp}_2\text{Re}_2(\text{CO})_3 \rightarrow \text{Cp}_2\text{Re}_2(\text{CO})_4 + \text{Cp}_2\text{Re}_2(\text{CO})_2$	58.3	64.7
$2\text{Cp}_2\text{Re}_2(\text{CO})_2 \rightarrow \text{Cp}_2\text{Re}_2(\text{CO})_3 + \text{Cp}_2\text{Re}_2(\text{CO})$	-4.7	5.7

Table 15. Dissociation Energies of the Binuclear Cyclopentadienylrhenium Carbonyls into Mononuclear Fragments (kcal/mol)

	MPW1PW91	BP86
$\text{Cp}_2\text{Re}_2(\text{CO})_5 \rightarrow \text{CpRe}(\text{CO})_3 + \text{CpRe}(\text{CO})_2$	33.3	31.2
$\text{Cp}_2\text{Re}_2(\text{CO})_4 \rightarrow \text{CpRe}(\text{CO})_3 + \text{CpRe}(\text{CO})$	52.2	54.1
$\text{Cp}_2\text{Re}_2(\text{CO})_4 \rightarrow 2\text{CpRe}(\text{CO})_2$	53.8	54.3
$\text{Cp}_2\text{Re}_2(\text{CO})_3 \rightarrow \text{CpRe}(\text{CO})_2 + \text{CpRe}(\text{CO})$	104.3	108.4
$\text{Cp}_2\text{Re}_2(\text{CO})_2 \rightarrow 2\text{CpRe}(\text{CO})$	96.5	97.8

Table 16. Energies (kcal/mol) for the Dissociation Of $\text{Cp}_2\text{Re}-\text{Re}(\text{CO})_n$ into $\text{Cp}_2\text{Re} + \text{Re}(\text{CO})_n$

	MPW1PW91	BP86
$\text{Cp}_2\text{Re}-\text{Re}(\text{CO})_5$ (5S-5) \rightarrow $\text{Cp}_2\text{Re} + \text{Re}(\text{CO})_5$	152.8	301.4
$\text{Cp}_2\text{Re}-\text{Re}(\text{CO})_4$ (4S-5) \rightarrow $\text{Cp}_2\text{Re} + \text{Re}(\text{CO})_4$	72.1	76.5
$\text{Cp}_2\text{Re}-\text{Re}(\text{CO})_3$ (3S-2) \rightarrow $\text{Cp}_2\text{Re} + \text{Re}(\text{CO})_3$	123.7	131.8
$\text{Cp}_2\text{Re}-\text{Re}(\text{CO})_2$ (2S-3) \rightarrow $\text{Cp}_2\text{Re} + \text{Re}(\text{CO})_2$	70.2	75.7

Table 17. Some Geometrical Parameters and Relative Energies of the Rhenocene Derivatives $\text{Cp}_2\text{Re}-\text{Re}(\text{CO})_n$ (BP86 results)

compound	agostic H-Re, Å ^a	Re-Re, Å	relative energy ^b (kcal/mol)
$\text{Cp}_2\text{Re}-\text{Re}(\text{CO})_5$ (5S-5)		3.183	46.4
$\text{Cp}_2\text{Re}-\text{Re}(\text{CO})_4$ (4S-5)	2.099 (1)	2.919	15.2
$\text{Cp}_2\text{Re}-\text{Re}(\text{CO})_3$ (3S-2)	2.553 (1)	2.652	23.6
$\text{Cp}_2\text{Re}-\text{Re}(\text{CO})_2$ (2S-3)	2.038 (2)	2.608	6.5
$\text{Cp}_2\text{Re}-\text{Re}(\text{CO})_2$ (2T-3)	2.676 (1), 2.723 (1)	2.621	18.5

^a The number of agostic hydrogen atoms is indicated in parentheses.^b Energy relative to the global minimum for $\text{Cp}_2\text{Re}_2(\text{CO})_n$.

electron-deficient metal atoms have been recognized in transition metal chemistry for more than 25 years.³⁹ However, rhenium compounds with agostic hydrogen atoms in C-H-Re bonds do not appear to have been reported.

Further loss of a carbonyl group from $\text{Cp}_2\text{Re}-\text{Re}(\text{CO})_4$ to give $\text{Cp}_2\text{Re}-\text{Re}(\text{CO})_3$ (**3S-2**) shortens the Re-Re distance further to 2.652 Å (BP86). This shortened bond distance would suggest a formal Re=Re triple bond. However, an unusual formal charge distribution of $\text{Cp}_2\text{Re}^{2+}=\text{Re}^{2-}(\text{CO})_3$

is required to give both rhenium atoms the favored 18-electron configuration. The C-H-Re agostic hydrogen interaction in **3S-2** is distinctly weaker than that in **4S-5**, since the Re-H distance in the C-H-Re bond increases to 2.553 Å.

Both singlet and triplet structures are known for the more highly unsaturated dicarbonyl $\text{Cp}_2\text{Re}-\text{Re}(\text{CO})_2$ with the two Cp rings bonded to the same rhenium atom (**III** in Figure 1). The singlet structure **2S-3** is significantly lower energy than the triplet structure **2T-3** (Table 17). The Re-Re distances of 2.608 Å and 2.621 Å for the singlet and triplet, respectively, represent very little shortening from the 2.652 Å Re-Re distance in the tricarbonyl $\text{Cp}_2\text{Re}-\text{Re}(\text{CO})_3$ (**3S-2**). The singlet structure $\text{Cp}_2\text{Re}-\text{Re}(\text{CO})_2$ (**2S-3**) has strongly bonded agostic hydrogens in C-H-Re bridges from each Cp ring, with Re-H distances of 2.038 Å. The bonding of the two agostic hydrogen atoms in the higher energy triplet $\text{Cp}_2\text{Re}-\text{Re}(\text{CO})_2$ structure **2T-3** is much weaker, as indicated by agostic Re-H distances of 2.676 Å and 2.723 Å.

4.2. Comparison of Analogous Rhenium and Manganese $\text{Cp}_2\text{M}_2(\text{CO})_n$ Derivatives. Table 18 compares the structures of analogous $\text{Cp}_2\text{M}_2(\text{CO})_n$ derivatives for rhenium and manganese. Only structures with one Cp ring bonded to each metal atom (**I** in Figure 1) are considered here since no structures of the type $\text{Cp}_2\text{M}-\text{M}(\text{CO})_n$ (**III** in Figure 1) are found for manganese. Note that for analogous structures the difference between the metal-metal distances for analogous rhenium and manganese derivatives ($\Delta(\text{Re}-\text{Mn})$) in Table 18) is approximately 0.2 Å in accord with the larger size of rhenium.

4.2.1 $\text{Cp}_2\text{M}_2(\text{CO})_5$. For both metals the lowest energy structures are singly bridged structures $\text{Cp}_2\text{M}_2(\text{CO})_4(\mu\text{-CO})$ with the *cis* isomer lying ~ 7 kcal/mol above the *trans* isomer. The *trans* isomer global minimum $\text{Cp}_2\text{Re}_2(\text{CO})_4(\mu\text{-CO})$ has been synthesized as a compound stable enough for structure determination by X-ray diffraction.⁷ However, the manganese analogue $\text{Cp}_2\text{Mn}_2(\text{CO})_4(\mu\text{-CO})$ has only been found as a transient intermediate in flash photolysis experiments, with a lifetime of ~ 0.1 s at room temperature.⁴⁰

4.2.2 $\text{Cp}_2\text{M}_2(\text{CO})_4$. For both metals the global minimum is an unbridged structure with a metal-metal distance suggesting the formal double bond required to give both metal atoms the favored 18-electron configuration. For both manganese and rhenium $\text{Cp}_2\text{M}_2(\text{CO})_4$ is thermodynamically unstable with respect to disproportionation into $\text{Cp}_2\text{M}_2(\text{CO})_5$

(39) Brookhart, M.; Green, M. L. H. *J. Organomet. Chem.* **1983**, 250, 395.(40) Creaven, B. S.; Dixon, A. J.; Kelly, J. M.; Long, C.; Poliakoff, M. *Organometallics* **1987**, 6, 2600.

Table 18. Comparison of the Structures (Distances in Å) and Energies (in kcal/mol) of Analogous Cyclopentadienylmanganese and Cyclopentadienylrhenium Carbonyl Derivatives $\text{Cp}_2\text{M}_2(\text{CO})_n$ (BP86 data)

structure and symmetry	M–M distance, Å			rel. energies, kcal/mol		bond order
	M=Mn	M=Re	$\Delta(\text{Re}–\text{Mn})$	M=Mn	M=Re	
$\text{Cp}_2\text{M}_2(\text{CO})_5$ structures						
$(\text{OC})_2\text{CpM}(\mu\text{-CO})\text{MCp}(\text{CO})_2$ (C_2)	2.804	3.017	0.213	0	0	1
$(\text{OC})_2\text{CpM}(\mu\text{-CO})\text{MCp}(\text{CO})_2$ (C_1)	2.846	3.064	0.218	7.4	7.3	1
$\text{Cp}_2\text{M}_2(\text{CO})_4$ structures						
$(\text{OC})_2\text{CpM}=\text{MCp}(\text{CO})_2$ (C_i)	2.509	2.752	0.243	0	0	2
$(\text{OC})\text{CpM}(\mu\text{-CO})_2\text{MCp}(\text{CO})$ (C_2)	2.505	2.808	0.303	3.8	5.2	2
$(\text{OC})_2\text{CpM}=\text{MCp}(\text{CO})_2$ (C_{2h})	2.457	2.648	0.191	1.0	11.0	2(triplet)
$\text{Cp}_2\text{M}_2(\text{CO})_3$ structures						
$\text{CpM}(\mu\text{-CO})_3\text{MCp}$ (C_2)	2.167	2.451	0.284	0	0	3
$(\text{OC})\text{CpM}(\mu\text{-CO})_2\text{MCp}$ (C_1 or C_s)	2.302	2.592	0.290	22.5	36.9	3(triplet)
$\text{Cp}_2\text{M}_2(\text{CO})_2$ structures						
$\text{CpM}(\mu\text{-CO})_2\text{MCp}$ (C_{2v})	2.202	2.490	0.188	0	4.3	3(triplet)
$\text{CpM}(\mu\text{-CO})_2\text{MCp}$ (C_s)	2.067	2.393	0.226	3.3	0	4

+ $\text{Cp}_2\text{M}_2(\text{CO})_3$ (see Table 14 for $\text{M}=\text{Re}$). Nevertheless, the permethylated derivative ($\eta^5\text{-Me}_5\text{C}_5$) $_2\text{Re}_2(\text{CO})_4$ can be synthesized by working under very mild conditions and is stable enough for structure determination by X-ray diffraction.⁸ However, ($\eta^5\text{-Me}_5\text{C}_5$) $_2\text{Re}_2(\text{CO})_4$ is very reactive with substrates such as CO and H_2 , even at -80°C , to give ($\eta^5\text{-Me}_5\text{C}_5$) $_2\text{Re}_2(\text{CO})_4(\mu\text{-CO})$ and ($\eta^5\text{-Me}_5\text{C}_5$) $_2\text{Re}_2(\text{CO})_4(\mu\text{-H})_2$, respectively.

The manganese triplet $(\text{OC})_2\text{CpMn}=\text{Mn}(\text{CO})_2$ lies only 1.0 kcal/mol above the singlet global minimum with a closely related structure. However, the corresponding rhenium triplet $(\text{OC})_2\text{CpRe}=\text{Re}(\text{CO})_2$ (**4T-2** in Figure 5) lies 11.0 kcal/mol above the corresponding global minimum. The higher energy of triplet electronic states of rhenium derivatives as compared with corresponding manganese derivatives may relate to the larger ligand field splittings in the rhenium complexes, particularly in structures of too low symmetry to have degenerate molecular orbitals required by group theory.

4.2.3 $\text{Cp}_2\text{M}_2(\text{CO})_3$. The triply bridged structures $\text{Cp}_2\text{M}_2(\mu\text{-CO})_3$ with formal $\text{M}\equiv\text{M}$ triple bonds have much lower energies than any other alternatives for both the manganese and rhenium derivatives. These structures correspond to stable compounds that have been isolated and characterized structurally by X-ray diffraction for both manganese^{41,42} and rhenium.⁹ The lowest-lying triplet structures are $\text{Cp}_2\text{M}_2(\text{CO})(\mu\text{-CO})_2$ with the manganese and rhenium derivatives lying 22.5 and 36.9 kcal/mol, respectively, above the $\text{Cp}_2\text{M}_2(\mu\text{-CO})_3$ global minima. Again, the larger ligand field splitting of rhenium leads to a higher relative energy for the triplet structures than in corresponding structures of its lighter congener manganese.

4.2.4 $\text{Cp}_2\text{M}_2(\text{CO})_2$. Both metals form relatively low energy singlet and triplet structures of the type $\text{Cp}_2\text{M}_2(\mu\text{-CO})_2$ with metal–metal distances suggesting formal quadruple and triple bonds, respectively, in accord with metal 18-electron configurations for the singlet structures and metal 17-electron

configurations for the triplet structures. However, at least with the BP86 method, the triplet structure is the global minimum for manganese, whereas the singlet structure is the global minimum for rhenium in accord with the trend noted above for $\text{Cp}_2\text{M}_2(\text{CO})_n$ ($n = 4, 3$).

5. Summary

The global minima found for $\text{Cp}_2\text{Re}_2(\text{CO})_n$ ($n = 5, 4, 3, 2$) using DFT methods all have structures similar to their manganese analogues. Thus, for $\text{Cp}_2\text{Re}_2(\text{CO})_5$ the predicted singly bridged $\text{Cp}_2\text{Re}_2(\text{CO})_4(\mu\text{-CO})$ structure with a formal Re–Re single bond is in close agreement with the known structure found by X-ray diffraction.⁷ For $\text{Cp}_2\text{Re}_2(\text{CO})_4$, the predicted doubly semibridged structure with a formal Re=Re double bond is again close to that of the known permethyl analogue ($\eta^5\text{-Me}_5\text{C}_5$) $_2\text{Re}_2(\text{CO})_4$. The latter, although highly reactive, is stable enough for structural characterization by X-ray diffraction.⁸ For $\text{Cp}_2\text{Re}_2(\text{CO})_3$, the predicted triply bridged structure with a formal Re \equiv Re triple bond is also very similar to the crystal structure of its very stable permethyl analogue⁹ ($\eta^5\text{-Me}_5\text{C}_5$) $_2\text{Re}(\mu\text{-CO})_3$. For $\text{Cp}_2\text{Re}_2(\text{CO})_2$, low energy doubly bridged singlet and triplet isomers have been predicted with metal–metal distances suggesting formal quadruple and triple bonds, respectively.

In addition to these structures with one Cp ring bonded to each metal (**I** in Figure 1), structures $\text{Cp}_2\text{Re}–\text{Re}(\text{CO})_n$, unknown in manganese chemistry, with both rings bonded to the same metal atom (**III** in Figure 1) have been found for rhenium, albeit at energies significantly above the global minima. The unsaturated $\text{Cp}_2\text{Re}–\text{Re}(\text{CO})_n$ ($n = 4, 3, 2$) structures have agostic Cp hydrogen atoms³⁹ forming C–H–Re bridges to the unsaturated $\text{Re}(\text{CO})_n$ group. This is a previously unrecognized feature in cyclopentadienylmetal carbonyl chemistry.

Acknowledgment. We are indebted to the 111 Project (B07012) in China and the U.S. National Science Foundation (Grants CHE-0749868 and CHE-0716718) for partial support of this work.

Supporting Information Available: Tables S1–S9: Theoretical harmonic vibrational frequencies for $\text{Cp}_2\text{Re}_2(\text{CO})_5$ (8 structures),

(41) Hermann, W. A.; Serrano, R.; Weichmann, J. J. *J. Organomet. Chem.* **1983**, *246*, C57.

(42) Bernal, I.; Korp, J. D.; Hermann, W. A.; Serrano, R. *Chem. Ber.* **1984**, *117*, 434.

$\text{Cp}_2\text{Re}_2(\text{CO})_4$ (12 structures), $\text{Cp}_2\text{Re}_2(\text{CO})_3$ (8 structures), and $\text{Cp}_2\text{Re}_2(\text{CO})_2$ (9 structures) using the BP86 method; Tables S10–S46: Theoretical Cartesian coordinates for $\text{Cp}_2\text{Re}_2(\text{CO})_5$ (8 structures), $\text{Cp}_2\text{Re}_2(\text{CO})_4$ (12 structures), $\text{Cp}_2\text{Re}_2(\text{CO})_3$ (8 structures) and $\text{Cp}_2\text{Re}_2(\text{CO})_2$ (9 structures) using the MPW1PW91

method; complete Gaussian 03 reference (ref 32, PDF). This material is available free of charge via the Internet at <http://pubs.acs.org>.

IC800403P